

Myocardial Positron Emission Computed Tomographic Images Obtained With Fluorine-18 Fluoro-2-Deoxyglucose Predict the Response of Idiopathic Dilated Cardiomyopathy Patients to Beta-Blockers

Shinji Hasegawa, MD, PhD,* Hideo Kusuoka, MD, PhD, FACC,† Kaoru Maruyama, MD, PhD,*
Tsunehiko Nishimura, MD, PhD,‡ Masatsugu Hori, MD, PhD, FACC,§ Jun Hatazawa, MD, PhD*
Suita, Osaka, and Kyoto, Japan

OBJECTIVES	The aim of this study was to elucidate whether the response of idiopathic dilated cardiomyopathy (DCM) patients to β -blockers can be predicted by positron emission tomography with fluorine-18 fluoro-2-deoxyglucose (FDG-PET).
BACKGROUND	Patients with DCM often have a poor prognosis, and it is important to predict their response to β -blocker therapy, which may be effective in DCM. However, no accurate methods of predicting their response have been available.
METHODS	In 22 DCM patients with reduced left ventricular (LV) systolic function, FDG-PET was performed. Uptake in the LV after glucose loading was evaluated based on the average global percent uptake of the injected dose (G%ID) and the coefficient of variance (CV) in 24 segments of the LV. Uptake during fasting was evaluated semiquantitatively on the basis of the total uptake score. The β -blocker was administered, and LV function was monitored by echocardiography. The histologic findings were assessed in the 18 patients who underwent endomyocardial biopsy.
RESULTS	The β -blocker was effective in the majority of patients whose G%ID after glucose loading was $>0.7\%$, and the sensitivity and specificity of G%ID as a predictor of β -blocker efficacy were 83.3% and 90.0%, respectively. Percent CV did not predict efficacy. Four groups, defined on the basis of the FDG uptake score during fasting and G%ID after glucose loading, had distinctive histologic findings and outcomes.
CONCLUSIONS	It has been shown that FDG-PET is a good predictor for the effectiveness of β -blockers. (J Am Coll Cardiol 2004;43:224-33) © 2004 by the American College of Cardiology Foundation

Metabolic imaging provides information on damaged myocardial cells different from that provided by myocardial perfusion imaging, and it is important in assessing the status of heart failure (HF) (1). Myocardial positron emission tomography (PET) with fluorine-18 fluoro-2-deoxyglucose (FDG) has been used to assess myocardial viability in ischemic heart disease (2), and histologic alterations have also been reported to be predicted by FDG-PET findings (3). However, the utility of FDG-PET in heart disease other than ischemic heart disease has never been demonstrated. There have been a comparatively large number of reports on FDG-PET in hypertrophic cardiomyopathy. Although FDG accumulates in the hypertrophied myocardium in the fasting state, the glucose uptake in the glucose-loaded state is lower than in that in normal myocardium (4). By contrast, there have been only a few FDG-PET studies in idiopathic dilated cardiomyopathy (DCM). Some of

them have shown that FDG-PET is useful in differentiating between idiopathic DCM and ischemic cardiomyopathy (5) and that inhomogeneous glucose metabolism predicts a poor outcome in DCM (6).

Beta-blocker therapy has been recognized as an excellent treatment for HF, including DCM (7), and the prognosis of patients in whom β -blockers are ineffective is poor. Moreover, β -blockers may worsen HF in serious cases, and thus prudence must be exercised in prescribing them. Prediction of β -blocker efficacy could be useful in planning the treatment regimen of HF patients, and the histologic findings have been reported to be useful in predicting the response to β -blocker therapy and outcome of DCM (8,9). The present study was designed to evaluate myocardial FDG-PET as a method of predicting both the response to β -blocker therapy in patients with DCM and the histologic findings.

METHODS

Study population. Twenty-two patients with reduced left ventricular (LV) systolic function whose LV ejection fraction (LVEF) was <0.45 and who did not have significant coronary artery stenosis were recruited from Osaka Univer-

From the *Department of Tracer Kinetics and Nuclear Medicine, Osaka University Graduate School of Medicine, Suita; and †Vice Director General, Osaka National Hospital, Osaka; ‡Department of Radiology, Graduate School of Medical Science Kyoto Prefectural University of Medicine, Kyoto; and §Department of Internal Medicine and Therapeutics, Osaka University Graduate School of Medicine, Suita, Japan.

Manuscript received February 3, 2003; revised manuscript received September 5, 2003, accepted September 9, 2003.

Abbreviations and Acronyms

CV	= coefficient of variance
DCM	= dilated cardiomyopathy
FDG	= fluorine-18 fluoro-2-deoxyglucose
(G)%ID	= (global) percent uptake of injected dose per 100 g tissue
HCFI	= histopathologic contractility failure index
HF	= heart failure
LV	= left ventricle/ventricular
LVEF	= left ventricular ejection fraction
PET	= positron emission tomography
SPECT	= single-photon emission computed tomography

sity Hospital. All patients gave their informed consent to participate in the study. Patients with diabetes mellitus were excluded. There were 17 males and 5 females (mean age 41.2 ± 16.8 years). All patients underwent myocardial FDG-PET. Four of 22 patients had a history of hypertension; one patient had received doxorubicin therapy 15 years previously; and one patient had a history of aortic valve replacement for severe aortic regurgitation because of a bicuspid aortic valve. Because these complications alone could not explain the reduction in LV systolic function in these six patients, all 22 patients were diagnosed with idiopathic DCM. To obtain the normal FDG uptake values, four male volunteers were assessed by the same FDG-PET protocol.

In 17 of the patients, β -blocker administration was begun within five weeks (interval between FDG-PET and the start of β -blocker therapy: 13.8 ± 11.1 days [mean \pm SD]) before or after FDG-PET imaging, in addition to other conventional medical therapy, such as angiotensin-converting enzyme inhibitors and diuretics. In five patients, the β -blocker was started in other hospitals, and when the patients were transferred to our hospital for control of HF, the dose of β -blocker was increased. Carvedilol ($n = 18$) or metoprolol ($n = 4$) was administered at an initial dose of 1.25 (or 2.5) mg/day or 5 mg/day, and the dose was increased every week to a final dose of 20 (or 15) mg/day or 40 (or 60) mg/day.

The PET procedure. The FDG-PET study was performed according to the one-day, three-acquisition protocol indicated in Figure 1 (10), using a whole-body PET camera (SET-2400W [Headtome V], Shimadzu Medico Co.,

Kyoto, Japan). Images after overnight fasting (PET-1) and after oral glucose loading (PET-3) were acquired serially on the same day. The image for subtraction (PET-2) was acquired just before the second injection of FDG, and the true glucose-loading image was prepared by subtracting PET-2 from PET-3. The Headtome V has 32 rings, providing 63 tomographic slices at 3.125-mm intervals. The spatial resolution in the tomographic plane was 4-mm full-width half-maximum (FWHM) at the center, and the axial resolution was 5-mm FWHM. Transmission scanning with rotating germanium-68 line sources was first performed for attenuation correction. After the subject had fasted overnight for at least 12 h, 370 MBq of FDG was injected via an antecubital vein. Forty-five minutes later, the first emission scan (PET-1) was performed, and the patients were then allowed to have lunch. Within 30 min after lunch, 75 g of glucose was loaded orally, and another 370 MBq of FDG was injected. The second emission scan (PET-2) was performed before the second FDG injection, and the third emission scan (PET-3) was performed 45 min after the second FDG injection.

Analysis of FDG-PET findings. The transaxial tomographic FDG-PET images were reconstructed from emission data by filtered backprojection, using a ramp filter and a Butterworth convolution filter, and attenuation was corrected by transmission data. The true glucose-loading images were made by subtracting the PET-2 from PET-3 images, taking the physical decay of ^{18}F into consideration. The transaxial images were transformed into a series of short-axis, vertical long-axis, and horizontal long-axis images.

The short-axis images of true glucose loading were used to construct a polar map of the LV, and the map was divided into 24 segments (8 segments for each slice of the basal, mid, and apical ventricle). Segmental percent uptake of the injected dose per 100 g tissue (%ID), the indicator of FDG uptake after glucose loading in each segment, was quantitatively calculated as body weight (60 kg)-corrected %ID, according to the following equation:

$$\%ID = \frac{Ct \times 100}{Dose \times CF \times 60/BW} \times 100$$

where Ct is the myocardial tissue activity of FDG (cpm/ml); BW (kg) is the patient's body weight; Dose (MBq) is the dose of FDG injected; and CF is the calibration factor for MBq on the curie meter and for counts per minute per milliliter on the PET images. The calibration factor, as measured in our institution, was 2.61×10^5 (cpm/ml/MBq). Left ventricular global uptake (G%ID) was calculated as the average of 24 segmental %IDs, and the dispersion of distribution of FDG was expressed in the form of the coefficient of variance (CV) of 24 segmental %IDs (%CV = standard deviation [SD]/mean of segmental %IDs).

Whenever FDG uptake during fasting was as low as the counts of the cardiac pool, %ID during fasting could not be

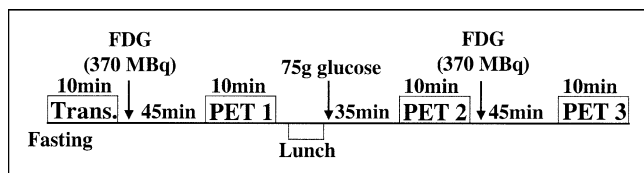


Figure 1. The one-day, three-acquisition protocol of fluorine-18 fluoro-2-deoxyglucose (FDG)-positron emission tomography (PET) for fasting and oral glucose loading. Images after overnight fasting (PET 1) and after oral glucose loading (PET 3) were acquired serially on the same day. The image for subtraction (PET 2) was acquired just before the second injection of FDG.

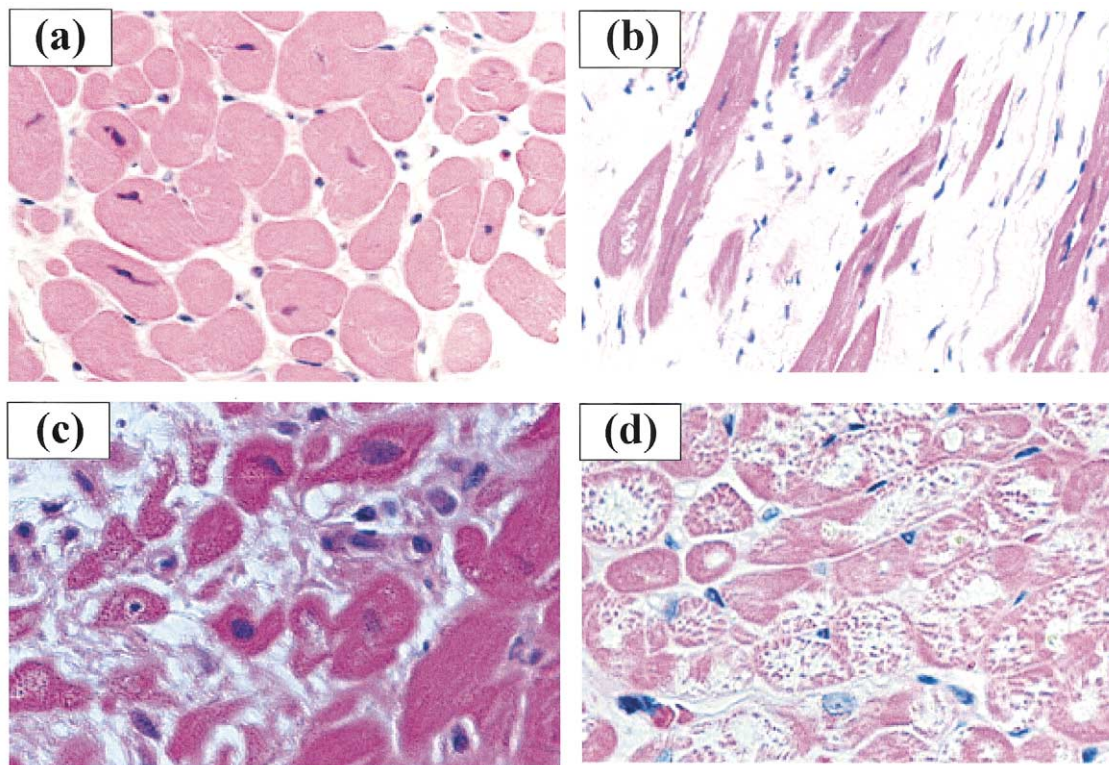


Figure 2. Typical examples of grading of the histologic findings (hematoxylin-eosin staining $\times 400$). (a) No fibrosis, no muscle bundle fragmentation, and no myocyte degeneration (histopathologic contractility failure index = 0). (b) Severe fibrosis but no degenerative change (scores: fibrosis = 3; fragmentation = 3; degeneration = 0). (c) Severe muscle bundle fragmentation but mild degeneration (scores: fibrosis = 2; fragmentation = 3; degeneration = 1). (d) Severe degeneration but no fibrosis (scores: fibrosis = 0; fragmentation = 0; degeneration = 3).

calculated accurately from the polar map. For instance, the cases in which the uptake occurred only in the cardiac pool and not in the myocardium showed various %ID values, and those cases could not be differentiated from cases with low uptake in the myocardium during fasting. Therefore, FDG uptake during fasting was evaluated by the semiquantitative method. The LV myocardium on the PET images was divided into a total of 20 segments: 6 segments each on the basal, mid, and apical short-axis images and 2 apical segments on the central vertical long-axis image. Uptake was then scored from 0 (no uptake) to 3 (high uptake) points. Uptake of FDG in the fasting images was evaluated by the total uptake score, which was the sum of the points for all 20 segments.

Myocardial perfusion scintigraphy. In 19 of the 22 patients, single-photon emission computed tomography (SPECT) with technetium-99m-tetrofosmin ($n = 15$) or thallium-201 chloride ($^{201}\text{TlCl}$) ($n = 4$) was performed within six weeks of FDG-PET (interval between SPECT and PET: 11.4 ± 10.4 days). Technetium-99m-tetrofosmin (370 MBq) or $^{201}\text{TlCl}$ (111 MBq) was injected intravenously at rest, and the SPECT images were obtained 60 min or 10 min, respectively, after the injection. The images were acquired with a three-head gamma camera (GCA9300A/HG; Toshiba Medico Co., Tokyo, Japan) equipped with high-resolution, general-purpose collimators. Each image was reconstructed from projection data acquired

over a 360° elliptical orbit by the filtered backprojection method and was transformed into a series of short-axis, vertical long-axis, and horizontal long-axis images. The LV myocardium on the SPECT images was divided into 20 segments in a similar manner to the FDG-PET images during fasting. Myocardial perfusion was then scored: 0 (normal); 1 (slightly reduced); 2 (moderately reduced); 3 (severely reduced); or 4 (defect). Myocardial perfusion was evaluated on the basis of the total defect score, calculated as the sum of the scores for each of the 20 segments.

Follow-up echocardiography. The response to the β -blocker was evaluated by M-mode echocardiography. Echocardiography was performed before β -blocker therapy and about one year (12 ± 1.8 months; $n = 18$) after the start of β -blocker therapy, with four exceptions: in one patient it was stopped because of sinus arrest after four months; one patient who had a good response to the β -blocker was transferred to another hospital at five months; and two patients showed no response to the β -blocker, despite treatment for over two years. Left ventricular end-diastolic and end-systolic dimensions were recorded, and LVEF was calculated by the Teichholz method (11). Patients whose LVEF had improved by more than 0.1 at follow-up compared with before treatment were defined as “responders.”

Histologic analysis of myocardium. Coronary angiography, study of the cardiac pressure, and endomyocardial biopsy were performed in 18 of the 22 patients. In 15

Table 1. Characteristics of β -Blocker Responders and Nonresponders

	Responders (n = 12)	Nonresponders (n = 10)	p Value
Age (yrs)	38.9 \pm 13.6	43.9 \pm 20.4	NS
Gender (M/F)	(9/3)	(7/3)	
β -Blocker (carvedilol/metoprolol)	(8/4)	(10/0)	
Days required for dose-up of β -blocker	31.9 \pm 9.3 (n = 9)	56.5 \pm 25.5 (n = 6)	<0.05
During fasting			
Plasma glucose (mg/dl)	93.2 \pm 8.3	99.2 \pm 9.3	NS
IRI (μ U/ml)	7.3 \pm 5.4	3.7 \pm 3.2	NS
Free fatty acids (μ Eq/l)	369.3 \pm 175.3	359.5 \pm 190.7	NS
After glucose loading			
Plasma glucose (mg/dl)	194.1 \pm 33.0	192.6 \pm 49.8	NS
IRI (μ U/ml)	107.9 \pm 55.5 (n = 10)	97.1 \pm 42.2 (n = 9)	NS
Free fatty acids (μ Eq/l)	161.0 \pm 137.4 (n = 6)	104.5 \pm 45.9 (n = 6)	NS
Noradrenaline (ng/ml)	0.51 \pm 0.39 (n = 6)	0.37 \pm 0.21 (n = 9)	NS
PCWP (mm Hg)	9.0 \pm 6.4 (n = 10)	15.5 \pm 6.5 (n = 8)	<0.05
CI (l/min per m ²)	2.9 \pm 0.9 (n = 11)	2.8 \pm 1.1 (n = 8)	NS
Systolic blood pressure (mm Hg)	104.3 \pm 16.0	98.2 \pm 16.3	NS
Diastolic blood pressure (mm Hg)	66.2 \pm 10.0	60.6 \pm 9.9	NS
Heart rate (beats/min)	70.8 \pm 17.1	69.7 \pm 9.9	NS
Before β -blocker therapy			
LVDD (mm)	69.3 \pm 7.9	69.5 \pm 8.2	NS
LVDS (mm)	60.1 \pm 9.0	60.9 \pm 3.6	NS
LVEF	0.282 \pm 0.109	0.263 \pm 0.090	NS
%FS	14.4 \pm 5.2	12.7 \pm 4.9	NS
After β -blocker therapy			
LVDD (mm)	57.3 \pm 8.6	69.9 \pm 7.4	<0.05
LVDS (mm)	41.1 \pm 10.5	61.9 \pm 8.9	<0.05
LVEF	0.552 \pm 0.151	0.249 \pm 0.084	<0.05
%FS	29.3 \pm 9.0	11.8 \pm 4.4	<0.05

Data are presented as the mean value \pm SD or number of patients.

CI = cardiac index; %FS = percent fractional shortening; IRI = immunoreactive insulin; LVDD = left ventricular end-diastolic dimension; LVDS = left ventricular end-systolic dimension; LVEF = left ventricular ejection fraction; NS = not significant; PCWP = pulmonary capillary wedge pressure.

patients, the biopsy was performed within one month before or after FDG-PET (interval between FDG-PET and biopsy: 11.3 \pm 7.4 days); in two patients it was performed in other hospitals (4 and 6 months before FDG-PET); and in one patient, the myocardial specimen was collected during LV assist device implantation about one year after FDG-PET. None of patients had any significant coronary artery stenosis. Significant stenosis was defined as stenosis >75% in major coronary arteries by the criteria of the American Heart Association. Asynergy in the apex was detected by left ventriculography in only one patient, but the lesion was concluded to be an infarction caused by thromboembolism from an LV thrombus, as the coronary artery was not atherosclerotic. The endomyocardial biopsy specimens were collected from the free wall of the LV with a biotome and an 8F-long sheath inserted into the LV via the femoral artery. The specimens were used for histologic analysis after hematoxylin-eosin staining. Five areas were examined in each specimen, and the histologic findings were evaluated on the basis of three pathologic features: fibrosis, muscle bundle fragmentation, and myocyte degeneration. Each of the histologic features was scored from 0 (no) to 3 (severe), and the scores were added to obtain the histopathologic contractility failure index (HCFI), as reported by Hirose (9) (Fig. 2).

Statistical analysis. Data are reported as the mean value \pm SD, and differences between the two groups (i.e., responders and nonresponders to β -blocker therapy) were assessed using the nonpaired *t* test. The likelihood of a response to the β -blocker was assessed by logistic regression analysis. Correlations between the parametric data and nonparametric data were assessed by the Spearman rank correlation test. Differences with a p value of <0.05 were considered statistically significant.

RESULTS

Response to β -blocker therapy. In 12 of the 22 subjects, the LVEF improved by more than 0.1 after β -blocker therapy, whereas in the other 10 patients, LVEF did not improve. By definition, the former and latter patients were responders and nonresponders, respectively. One patient in whom the β -blocker was stopped because of sinus arrest and one patient in whom the dose of the β -blocker could not be increased because of worsening of HF were included among the nonresponders. Table 1 summarizes the characteristics, drugs used for β -blocker therapy, laboratory data, and echocardiographic data of the responders and nonresponders. There were no significant differences in the

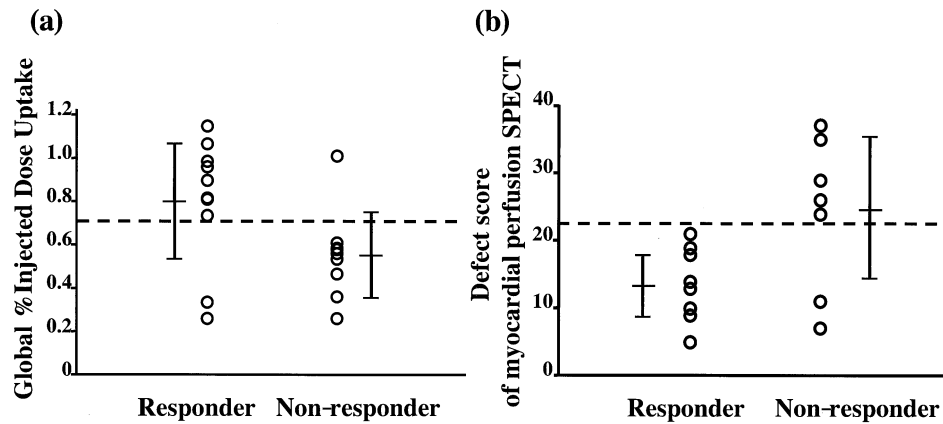


Figure 3. The (global) percent uptake of injected dose per 100 g tissue of fluorine-18 fluoro-2-deoxyglucose after glucose loading (a) and the total defect scores on the myocardial perfusion images (b) of responders and nonresponders. SPECT = single-photon emission computed tomography.

plasma levels of substrates and insulin between the two groups. The days required for dose-up of the β -blocker was significantly longer, and pulmonary artery wedge pressure was significantly higher in nonresponders than responders. All of the responders survived, but three the nonresponders died, one of whom received a heart transplant. There were no significant differences between responders and nonresponders in the echocardiographic data before β -blocker therapy. By contrast, the G%ID of FDG-PET after glucose loading was significantly higher in the responders ($0.80 \pm 0.27\%$) than in the nonresponders ($0.55 \pm 0.20\%$, $p < 0.05$; G%ID of normal volunteers: $0.83 \pm 0.15\%$) (Fig. 3a), and the total defect score on myocardial perfusion SPECT was lower in responders (13.2 ± 4.7) than in nonresponders (24.8 ± 10.7 , $p < 0.05$) (Fig. 3b). Single logistic regression analysis revealed that the G%ID of FDG after glucose loading ($p < 0.05$) and the total defect score of perfusion SPECT ($p < 0.05$) predicted the response to β -blocker therapy, but the echocardiographic parameters did not.

There were no significant differences between responders and nonresponders in the %CV of FDG-PET after glucose loading ($14.6 \pm 5.5\%$ vs. $19.0 \pm 10.6\%$, compared with normal subjects: $8.2 \pm 1.0\%$) or the total FDG-PET uptake scores during fasting (15.1 ± 17.5 vs. 19.0 ± 19.3). Assessment of the effectiveness of the β -blocker in the cases with G%ID $> 0.7\%$ of FDG after glucose loading revealed a sensitivity of 83.3% and a specificity of 90.0%. When β -blocker efficacy was assessed in cases with a total defect score on myocardial perfusion SPECT of < 22 , sensitivity was 100% and specificity was 75.0%. These best thresholds were determined by using receiver-operating characteristic (ROC) curves.

Relationship between FDG uptake and histologic findings in myocardium. None of the 18 patients who underwent myocardial biopsy had significant evidence of accumulation of inflammatory cells to make a diagnosis of acute myocarditis. Only one patient had myocardial disarray, but the patient did not have the specific pathologic findings of

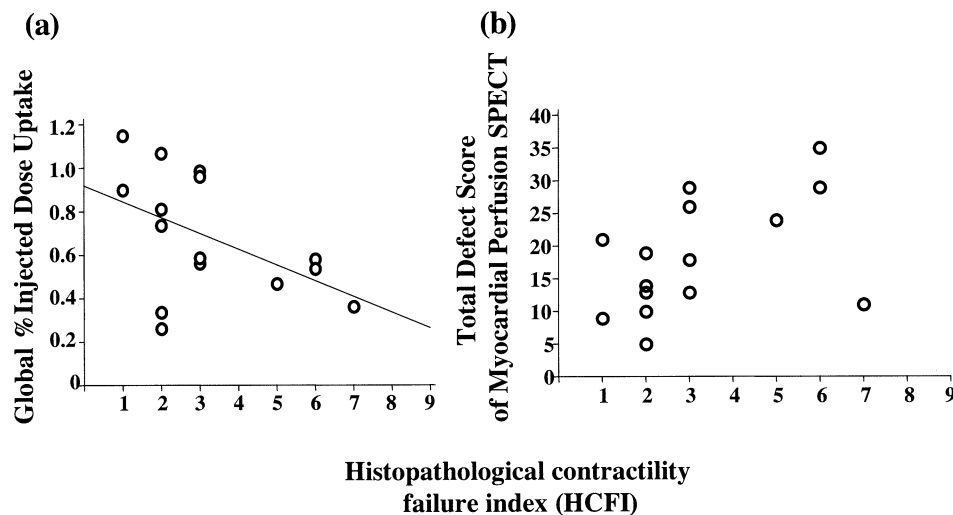


Figure 4. Relation of (global) percent uptake of injected dose per 100 g tissue of fluorine-18 fluoro-2-deoxyglucose on the glucose-loading image (a) and myocardial perfusion single-photon emission computed tomography (SPECT) total defect score (b) to histopathological contractility failure index as an index of histologic severity.

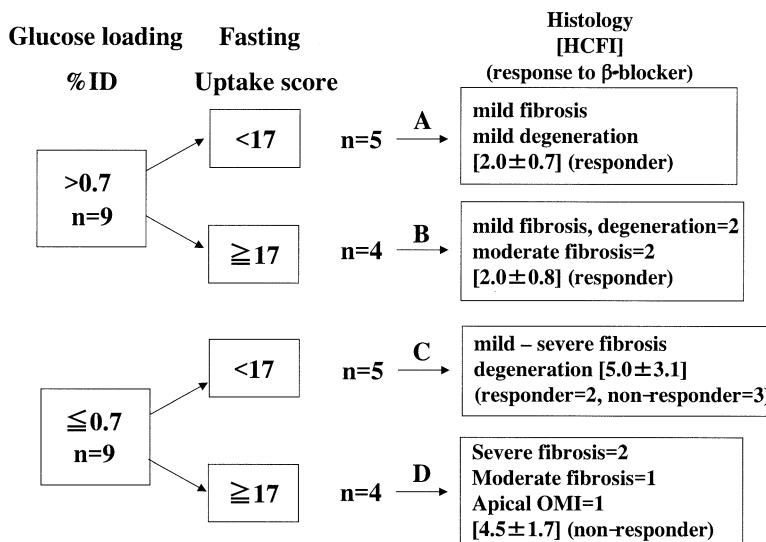


Figure 5. Relationship between fluorine-18 fluoro-2-deoxyglucose (FDG) uptake pattern and histologic findings. The patients were classified into four groups according to global percent of uptake of injected dose (ID) per 100 g tissue of FDG after glucose loading and total FDG uptake score during fasting. HCFI = histopathologic contractility failure index; OMI = old myocardial infarction.

hypertrophic cardiomyopathy. Little fibrosis was detected in six of the patients (fibrosis score = 0).

The G%ID of FDG in the glucose-loading image significantly correlated with the HCFI ($\rho = -0.53$, $p = 0.028$) (Fig. 4a). The G%ID was also significantly correlated with the fibrosis scores ($\rho = -0.52$, $p = 0.033$) and muscle bundle fragmentation scores ($\rho = -0.49$, $p = 0.045$). Although G%ID was not significantly correlated with the

myocyte degeneration scores ($\rho = -0.10$, $p = 0.679$), a few cases had low G%ID values despite exhibiting little fibrosis and severe degeneration. There was no relationship between the %CV of FDG after glucose loading and HCFI ($\rho = -0.03$, $p = 0.910$). As shown in Figure 4b, there were no significant correlations between the total defect score of myocardial perfusion SPECT and HCFI ($\rho = 0.49$, $p = 0.060$), nor were the total myocardial

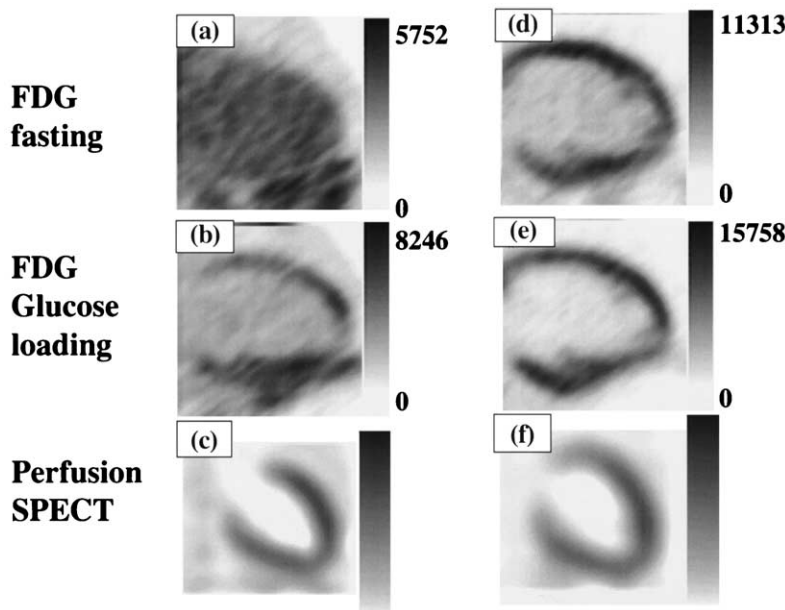


Figure 6. Vertical long-axis images in two cases of different types. The patient on the left side showed low fluorine-18 fluoro-2-deoxyglucose (FDG) uptake both during fasting (a) (total uptake score = 0) and after glucose loading (b) (global percent uptake of injected dose per 100 g tissue [G%ID] 0.36%), and a low myocardial perfusion defect score (c) (total defect score = 11). This patient had severe fibrosis (Fig. 7a), and the left ventricular ejection fraction did not improve after β -blocker therapy (from 0.20 to 0.20). The patient on the right side had high FDG uptake both during fasting (d) (total uptake score = 47) and after glucose loading (e) (G%ID 0.96%). Myocardial perfusion was also maintained (f) (total defect score = 13). Although dilation of the left ventricle was severe, the left ventricular ejection fraction was improved by the β -blocker (from 0.18 to 0.56) to the point where the patient became symptom-free. Histologic examination revealed severe myocyte degeneration and little fibrosis (Fig. 7b). SPECT = single-photon emission computed tomography.

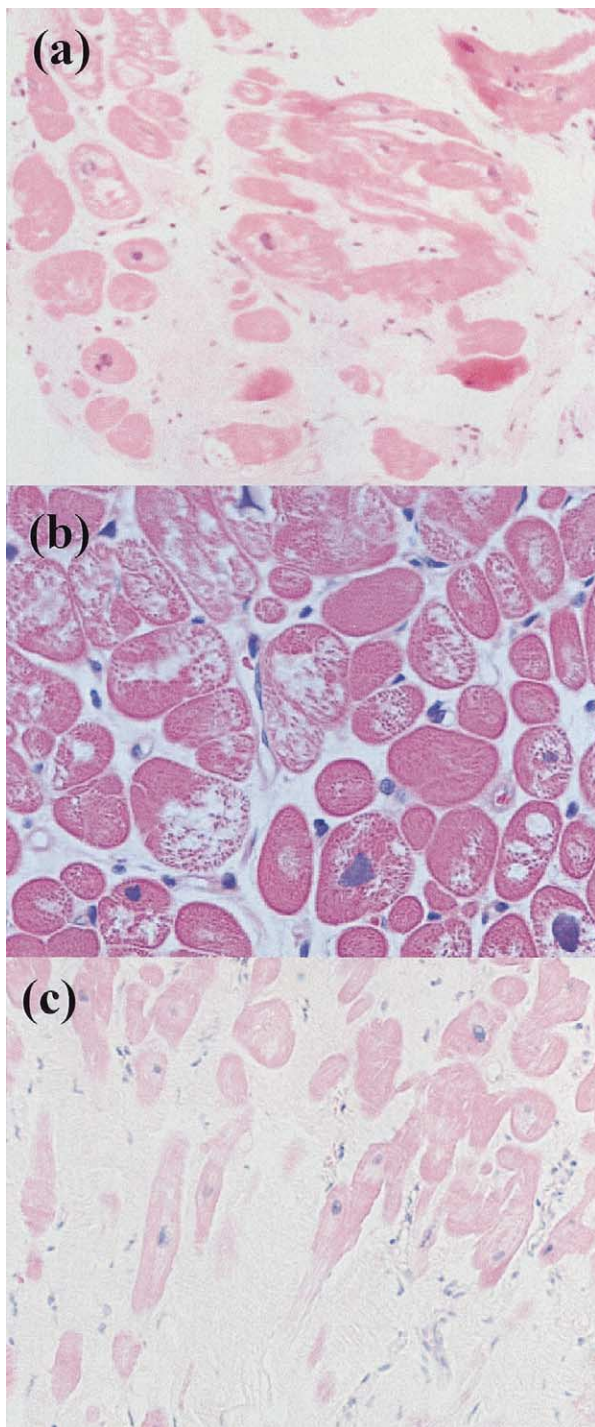


Figure 7. Histologic findings in the cases in Figures 6a to 6f, and 8. (a) Severe fibrosis and moderate degeneration. (b) No fibrosis and severe degeneration. (c) Severe fibrosis and mild degeneration (original magnification $\times 400$).

perfusion defect scores significantly correlated with the fibrosis, fragmentation, or degeneration scores. Figure 5 summarizes the relationship between the FDG uptake pattern and the histologic findings. The patients were classified into four groups (A to D), according to the G%ID

of FDG after glucose loading (patients were divided by the value defined from ROC analysis: 0.7%) and the total FDG uptake score during fasting (patients were divided by the mean value: 17) (Fig. 5). Each group had its own characteristic histologic findings.

DISCUSSION

Prediction of effectiveness of β -blocker therapy. The fibrotic pattern of the myocardium (8), serum brain natriuretic peptide concentration (12), and findings on nuclear medical imaging with ^{123}I -meta-iodobenzylguanidine (13) and ^{123}I -15-(p-iodophenyl)-3-R,S-methylpentadecanoic acid (14) have been reported as predictors of a response to β -blocker therapy in HF patients, and the results of the present study indicate that the G%ID of FDG after glucose loading is a good predictor of β -blocker efficacy in DCM patients. Yokoyama et al. (6) reported that FDG-PET findings predict cardiac events and improvement in LV function after medical therapy, including therapy with diuretics, digitalis, angiotensin-converting enzyme inhibitors, and β -blockers. They claimed that the %CV (i.e., index of dispersion) of the regional myocardial glucose utilization rate during oral glucose loading was the most important index predicting the outcome, but not the average regional myocardial glucose utilization rate. By contrast, in the current study, the %CV of the percent uptake of the dose injected after oral glucose loading did not predict the efficacy of β -blocker therapy. In our study, some patients with left bundle branch block who had a severe FDG defect in the septum and a high %CV value showed a good response. Some patients who had severe fibrosis showed diffuse low uptake and, as a result, a low %CV value. There were a few patients with slight fibrosis and severe generalized degeneration who did not respond to the β -blocker. These patients may have caused the discrepancy between the results of the two studies. It is difficult to evaluate the severity of a disease associated with diffuse damage, such as DCM, based on an index of dispersion, which reflects differences in regional damage.

It has been reported that perfusion SPECT is useful in predicting the outcome of DCM patients (15). In the current study, we found that the myocardial perfusion SPECT defect score, as well as the G%ID of FDG-PET, predicts the efficacy of β -blocker therapy. However, there were some discrepancies between the results of perfusion SPECT and FDG-PET. First, the perfusion SPECT defect score is supposed to indicate the extent of fibrosis (16). However, because the SPECT evaluations are relative, perfusion SPECT cannot accurately evaluate diffuse damage and may underestimate its severity. On the other hand, G%ID, which is not a relative value, was used in the assessment of FDG-PET. One patient with a low G%ID despite a low myocardial perfusion defect score did not improve, and his myocardium was replaced by diffuse fibrosis (Figs. 6a to 6c, and 7a). Uptake of FDG is affected

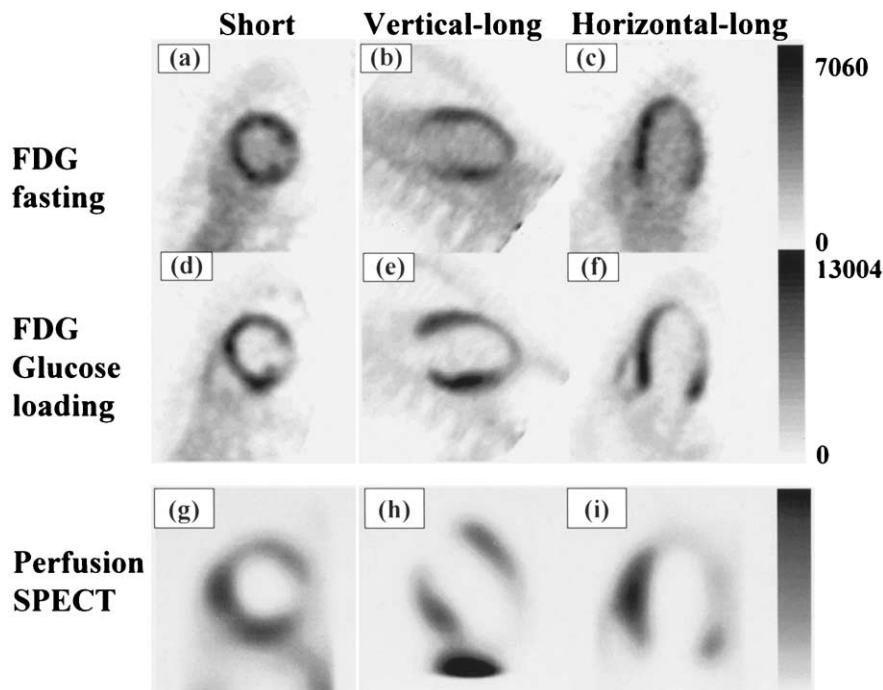


Figure 8. This patient had high fluorine-18 fluoro-2-deoxyglucose (FDG) uptake during fasting (**a to c**) (total uptake score = 33) and a broad, severely reduced region in the lateral wall on the glucose-loading image (**d to f**) (global percent uptake of injected dose per 100 g tissue 0.54). The findings on the perfusion single-photon emission computed tomography (SPECT) image (**g to i**) (total defect score = 35) were similar to those on the FDG-positron emission tomography image after glucose loading. Histologic analysis revealed severe fibrosis (Fig. 7c). The patient died of heart failure.

not only by myocardial fibrosis, but also by deterioration of glucose metabolism, such as glucose intolerance (10). Two patients who showed low FDG uptake, despite normal perfusion images, were good responders to β -blockers. The fibrosis is irreversible, but the reduced FDG uptake in such patients is not always irreversible.

The levels of plasma substrates and insulin are important factors affecting the uptake of FDG. We confirmed the absence of any significant differences in levels of glucose, free fatty acids, and insulin between responders and nonresponders. However, the insulin level was relatively high after glucose loading, and it has been reported that HF patients have insulin resistance and exhibit reactive hyperinsulinemia (17). In addition, in our study protocol, insulin levels were measured not only after 75-g oral glucose loading, but also after lunch. These factors may have been responsible for the increase in insulin level.

The FDG-PET study was performed more than one week after the start of β -blocker therapy in nine patients (β -blocker [+]: 4 responders, 5 nonresponders). There was no significant difference in G%ID after glucose loading between treated patients (β -blocker [+]; 0.52 ± 0.10) and the other patients (β -blocker [-]; 0.59 ± 0.27) in nonresponders ($p = 0.591$), whereas in responders, the G%ID of β -blocker (+) patients (0.59 ± 0.34) tended to be lower than that of β -blocker (-) patients (0.90 ± 0.15 , $p = 0.051$), but not statistically significantly. Wallhaus *et al.* (18) showed that glucose utilization remained unchanged after carvedilol treatment in congestive HF patients. However, in DCM patients, glucose metabolism might be enhanced by a

metabolic switch (19) and decreased by the beneficial effect of β -blocker therapy in responders.

Relationship between FDG-PET and histologic findings. Endomyocardial biopsy is performed in DCM patients not only to rule out secondary cardiomyopathy, such as cardiomyopathy secondary to amyloidosis, sarcoidosis, or myocarditis, but also to evaluate the severity of myocardial damage and predict the outcome (20). However, endomyocardial biopsy is invasive, and because the histologic findings are based on very small specimens, there is no way to know whether they are representative of the heart as a whole. We found that the severity of the histologic findings can be estimated by G%ID of FDG after glucose loading, and that the FDG accumulation pattern from fasting to glucose loading suggests the type of myocardial damage seen histologically. The FDG-PET study allows the state of the entire heart to be observed. For example, we were able to detect the regional damage in the lateral and antero-apical walls (Figs. 7c and 8).

A few reports have described glucose metabolism in the myocytes in DCM. Taylor *et al.* (21) reported that a higher myocardial fatty acid uptake rate in the failing heart is more than that expected in the normal heart, but with a lower myocardial glucose uptake rate. On the other hand, it has been reported that glucose utilization in HF increases even during fasting, the same as in an infant's heart (22). Actually, the results of the current study suggest that glucose uptake by myocytes in DCM is not uniform. We classified the subjects into four groups according to their FDG accumulation during fasting and after glucose loading.

In group A (Fig. 5), whose FDG uptake pattern was similar to that in normal myocardium, the histologic damage was mild and the systolic dysfunction was reversible. In group B, which showed accelerated uptake during fasting and maintenance of uptake after glucose loading, some patients had a fibrosis-dominant pattern, but it was milder than in group C, whereas other patients had little fibrosis and a large LV (Figs. 6d to 6f, and 7b). Presumably, the myocytes in the latter patients were in a state in which the cells were just able to survive, but their contractile function was impaired. It has been speculated that FDG uptake during fasting is increased due to strong wall stress by LV enlargement (23). Most of the patients in this group had a relatively good outcome. Group C, in which FDG uptake was reduced both during fasting and after glucose loading, comprised two subgroups. The first subgroup had diffuse severe fibrosis and severe degeneration of the remaining myocardium. One of two patients in this subgroup underwent heart transplantation, and the other (Figs. 6a to 6c, and 7a) is waiting for a heart transplant at the stage of New York Heart Association class III. The second subgroup had little fibrosis but showed severe degeneration. Although two of the patients in this subgroup were good responders to β -blockers, one of them died two years after FDG-PET. Many of the patients in group C showed discrepancies between their FDG-PET images after glucose loading and their myocardial perfusion SPECT images. The metabolic dysfunction in both subgroups apparently preceded the fibrosis. However, the metabolic dysfunction was fatal in some cases and not in others. In group D, which showed increased uptake during fasting, similar to ischemic myocardium, despite low global uptake after glucose loading, the fibrosis was severe. An example is shown in Figures 7c and 8. It was speculated that FDG accumulation increased in the remaining ischemic myocardium surrounded by fibrosis through a mechanism similar to that of the accumulation of FDG in myocardial infarction (24). Most patients in group D had intercellular fibrosis, as reported by Yamada et al. (8), and their diastolic function had deteriorated and resulted in a poor outcome despite their relatively small LV. In addition, some patients showed myocardial disarray and severe lysis or loss of myocytes, reported as post-myocarditis change. These findings suggest that the etiology in some of the patients group D might have been myocarditis (25).

Conclusions. Uptake of FDG after glucose loading was a good predictor of the response to β -blockers, and the FDG uptake patterns during fasting and after glucose loading provided some indication of the histologic findings.

Acknowledgments

We thank Dr. Reiko Doi for advice on the assessment of the histologic findings in the myocardium. We also thank Mr. Kouichi Fujino for technical support in regard to the PET acquisitions.

Reprint requests and correspondence: Dr. Shinji Hasegawa, Department of Tracer Kinetics and Nuclear Medicine, Osaka University Graduate School of Medicine, 2-2 Yamada-oka (D9), Suita, Osaka, Japan 565-0871. E-mail: hasegawa@tracer.med.osaka-u.ac.jp.

REFERENCES

1. Neglia D, Sambuceti G, Iozzo P, L'Abbate, Strauss HW. Myocardial metabolic and receptor imaging in idiopathic dilated cardiomyopathy. *Eur J Nucl Med* 2002;29:1403–13.
2. Tillisch J, Brunken R, Marshall R, et al. Reversibility of cardiac wall-motion abnormalities predicted by positron tomography. *N Engl J Med* 1986;314:884–8.
3. Maes A, Flameng W, Nuyts J, et al. Histological alterations in chronically hypoperfused myocardium—correlation with PET findings. *Circulation* 1994;90:735–45.
4. Uehara T, Ishida Y, Hayashida K, et al. Myocardial glucose metabolism in patients with hypertrophic cardiomyopathy: assessment by F-18-FDG PET study. *Ann Nucl Med* 1998;12:95–103.
5. Yamaguchi H, Hasegawa S, Yoshioka J, et al. Characteristics of myocardial ¹⁸F-fluorodeoxyglucose positron emission computed tomography in dilated cardiomyopathy and ischemic cardiomyopathy. *Ann Nucl Med* 2000;14:33–8.
6. Yokoyama I, Momomura S, Ohtake T, et al. Role of positron emission tomography using fluorine-18 fluoro-2-deoxyglucose in predicting improvement in left ventricular function in patients with idiopathic dilated cardiomyopathy. *Eur J Nucl Med* 1998;25:736–43.
7. Foody JM, Farrell MH, Krumholz HM. β -Blocker therapy in heart failure. *JAMA* 2002;287:883–9.
8. Yamada T, Fukunami M, Ohmori M, et al. Which subgroup of patients with dilated cardiomyopathy would benefit from long-term beta-blocker therapy? A histologic viewpoint. *J Am Coll Cardiol* 1993;21:628–33.
9. Hirose M. Evaluation of left ventricular function and prognosis in patients with idiopathic cardiomyopathy in comparison with endomyocardial biopsy findings with semiquantitative histopathological analysis—comparative study of hypertrophic and congestive (dilated) cardiomyopathy (in Japanese). *J Tokyo Wom Med Coll* 1982;52:292–306.
10. Hasegawa S, Kusuoka H, Uehara T, Yamaguchi H, Hori M, Nishimura T. Glucose tolerance and myocardial F-18 fluorodeoxyglucose uptake in normal regions in coronary heart disease patients. *Ann Nucl Med* 1998;12:363–8.
11. Teichholz LE, Kreulen T, Herman MV, Gorlin R. Problems in echocardiographic volume determinations: echocardiographic-angiographic correlations in the presence or absence of asynergy. *Am J Cardiol* 1976;37:7–11.
12. Stanek B, Frey B, Hulsmann M, et al. Prognostic evaluation of neurohumoral plasma levels before and during beta-blocker therapy in advanced left ventricular dysfunction. *J Am Coll Cardiol* 2001;38:436–42.
13. Fukuoka S, Hayashida K, Hirose Y, et al. Use of iodine-123 metaiodobenzylguanidine myocardial imaging to predict the effectiveness of beta-blocker therapy in patients with dilated cardiomyopathy. *Eur J Nucl Med* 1997;24:523–9.
14. Yoshinaga K, Tahara M, Torii H, Kihara K. Predicting the effects on patients with dilated cardiomyopathy of beta-blocker therapy, by using iodine-123 15-(p-iodophenyl)-3-R, S-methylpentadecanoic acid (BMIPP) myocardial scintigraphy. *Ann Nucl Med* 1998;12:341–7.
15. Tamai J, Nagata S, Nishimura T, et al. Hemodynamic and prognostic value of thallium-201 myocardial imaging in patients with dilated cardiomyopathy. *Int J Cardiol* 1989;24:219–24.
16. Watanabe M, Gotoh K, Nagashima K, et al. Relationship between thallium-201 myocardial SPECT and findings of endomyocardial biopsy specimens in dilated cardiomyopathy. *Ann Nucl Med* 2001;15:13–9.
17. Swan JW, Anker SD, Walton C, et al. Insulin resistance in chronic heart failure: relation to severity and etiology of heart failure. *J Am Coll Cardiol* 1997;30:527–32.

18. Wallhaus TR, Taylor M, DeGrado TR, et al. Myocardial free fatty acid and glucose use after carvedilol treatment in patients with congestive heart failure. *Circulation* 2001;103:2441–6.
19. van den Heuvel AFM, van Veldhuisen DJ, van der Wall EE, et al. Regional myocardial blood flow reserve impairment and metabolic changes suggesting myocardial ischemia in patients with idiopathic dilated cardiomyopathy. *J Am Coll Cardiol* 2000;35:19–28.
20. Billingham ME. Role of endomyocardial biopsy in diagnosis and treatment of heart disease. In: Silver MD, editor. *Cardiovascular Pathology*. 2nd ed. New York, NY: Churchill Livingstone, 1991; 1465–86.
21. Taylor M, Wallhaus TR, DeGrado TR, et al. An evaluation of myocardial fatty acid and glucose uptake using PET with [¹⁸F]fluoro-6-thia-heptadecanoic acid. *J Nucl Med* 2001;42:55–62.
22. Kelly DP, Gordon JI, Alpers R, Strauss AW. The tissue-specific expression and developmental regulation of two nuclear genes encoding rat mitochondrial proteins: medium chain acyl-CoA dehydrogenase and mitochondrial malate dehydrogenase. *J Biol Chem* 1989;264: 18921–5.
23. Batista RJ, Verde J, Nery P, et al. Partial left ventriculectomy to treat end-stage heart disease. *Ann Thorac Surg* 1997;64:634–8.
24. Fallavollita JA. Spatial heterogeneity in fasting and insulin-stimulated ¹⁸F-2-deoxyglucose uptake in pigs with hibernating myocardium. *Circulation* 2000;102:908–14.
25. Hasumi M, Sekiguchi M, Yu ZX, Hirosawa K, Hiroe M. Analysis of histopathologic findings in cases with dilated cardiomyopathy with special reference to formulating diagnostic criteria on the possibility of postmyocarditic change. *Jpn Circ J* 1986;50:1280–7.